

# Heat transfer analysis for high-flux solar measurements using a flat plate calorimeter

M. Mouzouris, L. W. Roberts and M. J. Brooks

School of Mechanical Engineering, University of KwaZulu-Natal, Durban, 4041, South Africa

Centre for Renewable and Sustainable Energy Studies

## Abstract

A novel point-focus solar concentrator has been developed to provide thermal energy requirements for high temperature terrestrial and space applications. The optical system is known as the Fibre Optic Concentrating Utilisation System (FOCUS) and comprises a 600 mm diameter composite material ring array concentrator, designed to inject solar rays into a fibre optic bundle. Transmission of the concentrated solar radiation via optical fibres facilitates energy use by separating the collector from its remote target. A realistic performance analysis of the overall system based on ray trace methods shows an expected maximum power density of  $133.9 \text{ W/cm}^2$  at fibre optic exit. A flat plate calorimeter was constructed to measure the concentrated solar energy at cable exit for comparison with simulation results. The calorimeter consists of a stainless steel body that houses a 60 mm diameter copper plate to receive concentrated solar energy. The copper plate is supported with Ertalon 66SA Polyamide to minimise heat transfer between the plate and calorimeter body. This paper discusses the performance of FOCUS using a ray trace exercise and heat transfer analysis in the calorimeter based on energy balance methods. Energy absorbed by the water flow and external losses due to convection and radiation are described.

*Keywords:* point-focus concentrator, fibre optic bundle, heat transfer, flat plate calorimeter, high-flux measurements.

## 1. Introduction

Point-focus solar collectors have been used for applications such as electricity production, hydrogen generation (Pregger, et al., 2008) and lunar in-situ resource utilisation (ISRU) research (Nakamura and Senior, 2008). To date, parabolic dishes have largely been used for point-focus applications, however other options exist. A novel multi-element concentrator design developed by Vasylyev and Vasylyev (2002) provides high concentration of energy with single stage reflection. The concentrator design called a ring array concentrator (RAC) consists of a set of paraboloidal ring elements to converge incident solar energy to a common focus. The advantage of using the RAC design over the dish is the benefit of its rear focusing characteristic. This feature eliminates the need for a Cassagrain-type design where the rays are re-focused downward and facilitates integration with the support structure to receive concentrated solar energy.

The use of highly concentrated energy is limited if it can only be harnessed at the concentrators' focal point. For this reason studies have been demonstrated integrating solar concentrators with fibre optic cables for energy transmission to a remote target (Kribus et al., 2000). An example of such a system is the solar fibre optic mini-dish concentrator developed by Feuermann and Gordon (2002) for solar surgery applications.

This research describes a solar concentrating system developed at the University of KwaZulu-Natal called the Fibre Optic Concentrating Utilisation System (FOCUS). Key system components comprise a composite material ring array concentrator designed to inject incident

solar rays into a fibre optic bundle. The system is intended for use in a ISRU program where high-flux concentrations are required.

The measurement of high-flux solar energy is required to characterise the performance of a solar concentrating system. Several devices have been developed for high-flux solar measurements, including calorimetric and radiometric techniques (Ballestrín et al., 2006). Calorimeters use energy balance methods to obtain estimated flux concentrations incident on the receiving surface. The methodology includes determining the heat absorbed by a heat transfer fluid flowing through the calorimeter body, by measuring the change in temperatures at inlet and outlet (Estrada et al., 2007). Considerations for this technique include minimising uncertain measurements pertaining to mass flow rate of the fluid and rise in temperature at calorimeter exit. Estimated modeling of heat losses due to convection and radiation is needed when the receiver plate does not approximate ambient temperature. Other devices used for measuring heat flux are radiometers, such as the Gardon Gage (Ballestrin et al., 2003). Operating principles include measuring the radial temperature difference of a circular foil disk using a differential thermocouple. The disk is machined from constantan and attached to a cylindrical copper heat sink. Material properties of the assembly produce a 10mV maximum output that is directly proportional to the absorbed heat flux. A combination of calorimetric and radiometric methods can also be employed to measure concentrated solar radiation (Pérez-Rábago et al., 2006). The device operates as a normal radiometer and a calorimetric component is added to calibrate the apparatus.

This paper discusses the construction of a flat plate calorimeter for determining the high-flux solar measurements of FOCUS. Energy balance methods include using the simplified steady-flow thermal energy equation to estimate the heat absorbed by the circulating fluid. Heat loss modeling due to convection and radiation are described. Experimental results will be compared to theoretical ray trace simulations during the performance testing programme.

## 2. Solar thermal system

FOCUS was developed to supply thermal power to a variety of high temperature processes, including lunar ISRU applications. A minimum design flux of  $85 \text{ W/cm}^2$  is specified (Mouzouris and Brooks, 2009) at fibre optic cable exit, with the intention of melting the lunar regolith simulant JSC 1-A for lunar materials processing. Potential terrestrial applications include hydrogen generation and solar-powered refrigeration systems such as those described by du Clou et al. (2010). The optical system comprises a composite material ring array concentrator, a high numerical aperture fibre optic cable and a dual axis solar tracker (Fig. 1).



**Figure 1. The Fibre Optic Concentrating Utilisation System developed for high temperature applications. Preliminary testing at the 20 mm diameter concentrator focal point achieved temperatures exceeding  $1400^{\circ}\text{C}$ .**

## 2.1 Composite material RAC

The 600 mm diameter composite material ring array concentrator consists of seven reflective elements and is housed in a rigid aluminium framework (Fig. 2). Each element has a different paraboloidal geometry designed to focus direct normal irradiation to a common point. Construction of the reflective elements includes the use of composite materials and a mold as described by Mouzouris and Brooks (2010). Optical characterisation of the elements is necessary to quantify the composite material manufacturing method. A co-ordinate measuring machine (CMM) was used to measure surface contours for each element (Kumler and Caldwell, 2007). The CMM provides scanned profiles of the reflective surface for each ring element before processing the results to obtain slope error. Results from the slope error analysis are tabulated in Table 1. Slope errors between 5.67 mrad and 2.90 mrad root mean square (rms) were observed. The general trends of the errors show an increase in accuracy with the smaller diameter elements and vice versa. The slope error results suggest that ring array designs should ideally comprise reflective elements with reduced curvatures if composite material methods are employed.

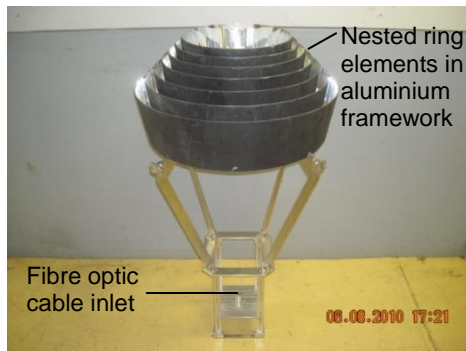


**Figure 2. Composite material RAC housed in an aluminium support framework.**

**Table 1. Slope error results for characterising reflective elements. Root mean square error (RMSE) for each element includes a sample of 392 observations.**

Ring element	RMSE (mrad)
1	4.77
2	5.67
3	5.39
4	4.02
5	3.32
6	1.22
7	2.90

## 2.2 Fibre optic cable

The fibre optic cable is manufactured by CeramOptec and consists of a 0.37 numerical aperture bundle of 900 silica fibres treated to resist UV degradation. The bundle is 4 meters in length with transmission efficiency of 95%. It has a 6 mm diameter fused inlet end and an 8.2 mm diameter unfused outlet. The fused inlet lowers injection losses by reducing the spacing between each fibre.

## 2.3 Dual axis solar tracker

A dual axis tracker is required for point focus systems to minimise the optical loss that occurs when incident light deviates from the aperture normal. The tracking system to be used in this research is manufactured by Small Power Systems and has an accuracy of  $0.05^\circ$ . A ray trace analysis was conducted in previous work (Mouzouris and Brooks, 2009) to quantify the performance of the system with a maximum tracking error on the RAC. Results show that the 600 mm diameter RAC performs at 97% its ideal performance when  $0.05^\circ$  misalignment is introduced. Further system ray tracing exercises includes incorporating surface slope errors into simulations.

### 3. Ray tracing results

A computational analysis was conducted to predict performance results of the composite material concentrator using ray tracing software (OptisWorks Studio). An optical model of the solar thermal system, utilising the error results obtained by 3D surface mapping, was developed and the overall optical efficiency of FOCUS was estimated.

Ideal and real simulations of the system were conducted at an irradiance value of  $850 \text{ W/m}^2$  to obtain comparative power density results. Ideal parameters include parallel rays of sunlight incident on the ideal RAC and perfect specular reflection from the elements. Realistic parameters incorporate the solar half angle of  $0.255^\circ$ , 95% specular reflection for the reflective surface, a maximum tracking error of  $0.05^\circ$  and a worst case representative sample of the surface slope errors for each manufactured element.

Results from the ray tracing exercise are shown in Figure 3. Average power densities incident on the fibre optic cable of  $557.86 \text{ W/cm}^2$  and  $165.13 \text{ W/cm}^2$  ( $\dot{q}_{theo,in}$ ) were observed for the ideal and real simulations respectively. After injection and transmission through the cable an ideal flux level of  $453.95 \text{ W/cm}^2$  was calculated. A realistic flux at cable exit,  $\dot{q}_{theo,out}$  of  $133.94 \text{ W/cm}^2$  was observed that exceeds the specified design value by 158%, suggesting FOCUS is capable of sintering lunar regolith for ISRU processes. Overall optical efficiency of 81% and 24% were calculated for the ideal and real cases respectively. An experimental test programme will be conducted to verify the flux and efficiency results obtained in the realistic simulation.

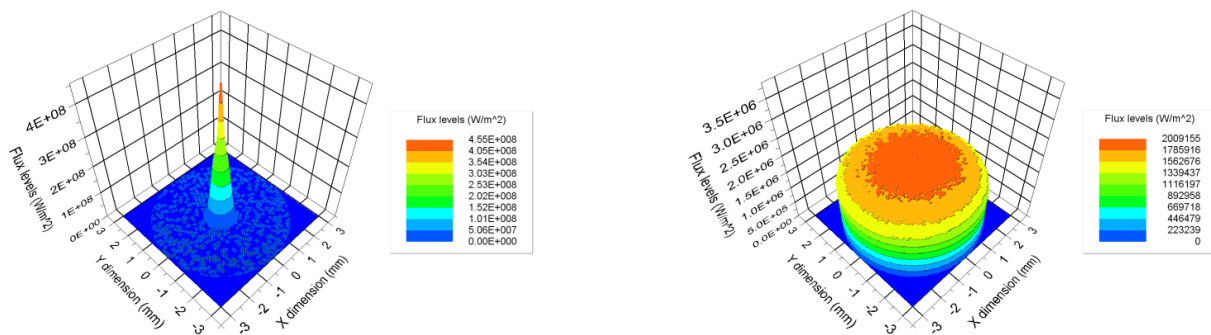


**Figure 3. Three dimensional flux maps showing ideal (left) and realistic (right) simulations at the 6 mm diameter inlet to the fibre optic cable. The ideal simulation shows point convergence of sunlight within an area of diameter 1.3 mm. The realistic result shows a more uniform distribution of energy with a slight center offset due to the tracking error.**

### 4. Heat transfer analysis

In order to validate the theoretical ray tracing performance results, a flat plate calorimeter was constructed to measure the high-flux solar measurements of FOCUS. The experimental aim is to quantify the power densities at inlet and exit of the fibre optic cable by energy balance methods. The calorimeter design is based on work done by Jaramillo et al. (2008).

#### 4.1 Calorimeter construction

The calorimeter with its sub-components is shown in Figure 4. The cylindrical outer casing is machined from stainless steel that houses a nylon insulator, radial flow distributor and a copper receiver. The insulation material is Ertalon 66SA Polyamide which minimises heat transfer between the calorimeter body and water flow. It has a low thermal conductivity of  $0.25 \text{ W/(m.K)}$ .

The radial flow distributor threads into the cylindrical water passage and allows water to diffuse evenly on to the copper disc. The 60 mm diameter copper plate of 6 mm thickness fastens on to the insulation and concentrically covers the distributor with a gap that allows water flow. The copper surface exposed to the concentrated energy is painted with a black absorbing coat to increase energy absorption.

The operational procedure involves concentrated rays striking the copper disc while cold water flows through the device to absorb energy. Cold water enters via the inlet and flows up the water passage arriving at the copper receiver where heat transfer takes place. The water contacts the inner surface of the copper thereby removing heat before flowing radially between the plate and distributor to exit the device. An energy balance is carried out on the copper disc to determine the concentrated flux arriving at the plate surface.

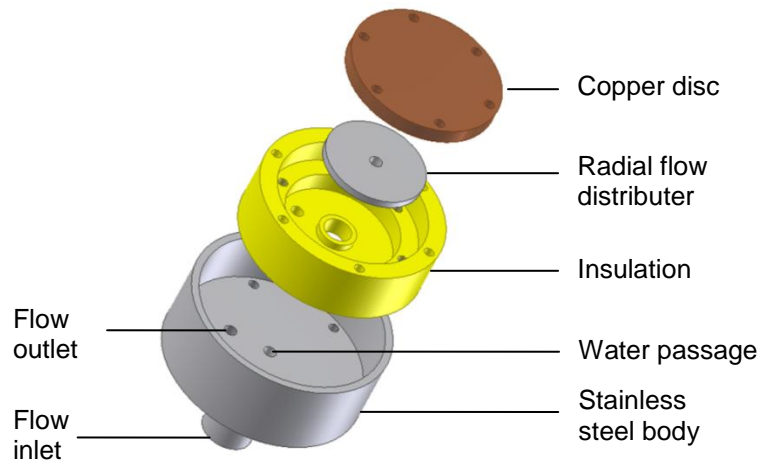


**Figure 4. Exploded view of the flat plate calorimeter constructed for performance measurements of FOCUS. The device consists of a cylindrical stainless steel outer casing that houses a nylon insulator, a radial flow distributor and the copper receiving plate.**

#### 4.2 Energy balance

The conservation of energy derived from the first law of thermodynamics is required to carry out energy balance calculations (Incropera et al., 2007). The methodology includes defining a control volume, identifying relevant heat transfer processes and establishing the rate equations. The general form of conservation of energy states that on a rate basis, the stored energy,  $\dot{E}_{st}$ , equals the energy inflow,  $\dot{E}_{in}$  plus the thermal energy generated,  $\dot{E}_g$ , minus the energy outflow,  $\dot{E}_{out}$  (eq. 1). Under assumed steady state conditions there is no change in energy storage, and due to zero thermal energy generated, Equation 1 is simplified to zero change in energy inflow and outflow (eq. 2).

$$\dot{E}_{in} + \dot{E}_g - \dot{E}_{out} = \dot{E}_{st} \quad (1)$$

$$\dot{E}_{in} - \dot{E}_{out} = 0 \quad (2)$$

Figure 5 illustrates the control volume around the copper receiver as the boundary where energy inflow and outflow occurs. The aim of the energy balance is to estimate the solar power incident on the plate,  $q_{in}$ , by summing the energy absorbed by the water flow,  $q_{abs}$  and the external heat losses,  $q_{l,out}$  (eq. 3). The absorptivity of the plate surface,  $\alpha_s$  estimates the

fraction of incident irradiation absorbed. Internal losses are neglected due to the nylon insulation inside the calorimeter body.

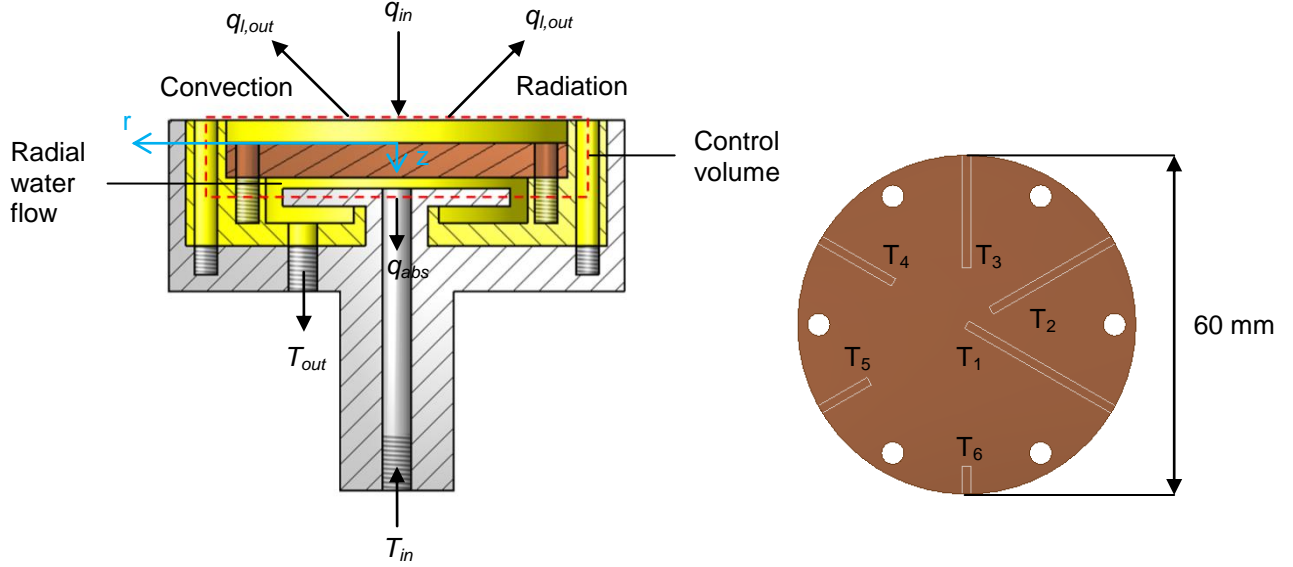


**Figure 5. (left) Calorimeter cross-section illustrating the conservation of energy for a steady-flow, open system. (right) Top view of the six thermocouple positions inside the copper plate, starting with  $T_1$  at  $r = 0$  mm, increasing anti-clockwise in increments of 5 mm, ending with  $T_6$  at  $r = 25$  mm.**

$$\alpha_s q_{in} = q_{abs} + q_{l,out} \quad (3)$$

Energy absorbed by the water flow is estimated by the simplified steady-flow thermal energy equation (eq. 4), where  $\dot{m}$  is the mass flow rate,  $C_{p,w}$  is the specific heat of water and  $T_{out}$  and  $T_{in}$  are the water outlet and inlet temperatures respectively. External heat losses to the surroundings arise from convection,  $q_{conv}$  and radiation,  $q_{rad}$  at the copper plate surface (eq. 5), where  $A_{Cu}$  is the area of the copper plate,  $h$  is the convective heat transfer co-efficient at the surface,  $\varepsilon_s$  is the emissivity of the plate,  $\sigma$  is the Stefan-Boltzmann constant and  $T_s$  and  $T_{amb}$  are the mean value of surface temperature and ambient temperature, respectively. To approximate a mean temperature value at a depth of  $z = 3$  mm, six thermocouples, equidistant apart are radially positioned (Fig. 5). The thermocouples will measure radial temperature distribution midway in the plate. To obtain a mean temperature at the plate surface, a conduction analysis in the  $z$ -direction is modeled to approximate the additional temperature from  $z = 3$  mm to the plate surface ( $z = 0$  mm). Using ray tracing results the temperature change,  $\Delta T$  between the top ( $z = 0$  mm) and bottom ( $z = 6$  mm) surfaces of the plate can be estimated with Equation 6, where  $\alpha_s \check{q}_{theo,in}$  is the heat flux in the  $z$ -direction,  $k$  is the thermal conductivity of copper and  $t$  is the plate thickness. Halving the temperature change estimates the temperature difference in the  $z$ -direction from  $z = 3$  mm to the plate surface ( $z = 0$  mm), where concentrated solar rays strike.

$$q_{abs} = \dot{m} C_{p,w} (T_{out} - T_{in}) \quad (4)$$

$$q_{l,out} = q_{conv} + q_{rad} \quad (5)$$

$$= A_{Cu} [h(T_s - T_{amb}) + \varepsilon_s \sigma (T_s^4 - T_{amb}^4)]$$

$$\alpha_s \check{q}_{theo,in} = k \frac{\Delta T}{t} \quad (6)$$

### 4.3 Experimental setup

The experimental procedure to determine high-flux solar measurements includes positioning the calorimeter firstly at the focal point of the concentrator, and secondly at fibre optic cable exit. At concentrator focus, a reflective shield with a 6 mm diameter opening will cover the calorimeter to represent the cable inlet. A fibre optic cable exit flux value will be determined by positioning the concentrated energy directly on to the calorimeter. Concentric solar radiation incident on the center of the calorimeter is assumed. Results from both experiments will be compared to theoretical ray tracing simulations.

Key components of the experiment include FOCUS, the calorimeter, water pumping system and instrumentation. The fluid circulation system consists of a pump fitted with throttling valves to obtain the desired mass flow rate. The flow rate is set to keep the copper receiving plate at a temperature close to ambient to minimise external heat losses due to convection and radiation. Instrumentation includes two type T thermocouples for the inlet and outlet water measurements and six type K thermocouples for the temperature distribution measurements midway in the copper plate. Data acquisition software was developed in LabVIEW to log results for readings.

The testing procedure includes logging measurements at various irradiance values. The proposed running time is three minutes per test, which assumes steady state water flow and negligible differences in direct normal irradiation. Proposed parameters, temperatures and expected results for the heat transfer analysis are given in Table 2 for comparison with the ray tracing simulations. Absorptivity and emissivity values represent an estimated value for the copper surface coating. Mass flow rate was chosen to induce turbulent flow for uniform mixing in the device and the convective heat transfer co-efficient is reported by Jaramillo et al. (2008). As an example of the operation of the energy model, a set of temperatures was assumed for the copper plate and the water flowing through the calorimeter at inlet and outlet. These temperatures were then used to predict the incident solar flux on the copper plate using the energy balance of Equation 3. For the chosen parameters, the model predicts a flux of 233.9 W/cm<sup>2</sup> at cable inlet ( $\dot{q}_{exp,in}$ ) which exceeds the predicted ray trace value,  $\dot{q}_{theo,in}$  of 165.13 W/cm<sup>2</sup> by 142%. This suggests that either the assumed temperatures are slightly too high, or the ray tracing model is overly conservative. A possible reason for underestimating performance in the ray trace analysis is the assumption of an optical worst case scenario for each reflective element. The expected results from energy balance methods suggest a fibre optic exit flux value,  $\dot{q}_{exp,out}$  of 188.9 W/cm<sup>2</sup>. The FOCUS testing programme will commence in November 2010 and aims to compare ray tracing simulations with experimental results.

Table 2. Proposed parameters, predicted temperature values and expected results for energy balance calculations.

Proposed parameter values		Predicted temperature values (K)		Model results based on predicted temperatures	
$\alpha_s$	0.95	$T_{in}$	298	$q_{in}$ (W)	66.1
$\epsilon_s$	0.85	$T_{out}$	301	$q_{abs}$ (W)	62.7
$\dot{m}$ (kg/s)	$5.0 \times 10^{-3}$	$T_0$	360	$q_{l,out}$ (W)	0.12
$C_{p,w}$ (J/kg.K)	4180	$T_5$	350	$\dot{q}_{exp,in}$ (W/cm <sup>2</sup> )	233.9
$A_{Cu}$ (m <sup>2</sup> )	$2.83 \times 10^{-5}$	$T_{10}$	340	$\dot{q}_{exp,out}$ (W/cm <sup>2</sup> )	188.9
$h$ (W/m <sup>2</sup> .K)	80	$T_{15}$	330		
$\sigma$ (W/m <sup>2</sup> .K <sup>4</sup> )	$5.670 \times 10^{-8}$	$T_{20}$	320		
$k$ (W/m.K)	401	$T_{25}$	310		
$t$ (mm)	6	$T_{amb}$	298		
$\dot{q}_{theo,in}$ (W/cm <sup>2</sup> )	165.13	$T_s$	347		
$\dot{q}_{theo,out}$ (W/cm <sup>2</sup> )	133.94	$\Delta T$	23.5		

## 5. Conclusion

A point-focus solar concentrating unit known as the Fibre Optic Concentrating Utilisation System (FOCUS) has been designed to provide thermal energy for a variety of high heat flux applications, including lunar materials processing. Key components of FOCUS include a ring array concentrator comprising a nested set of reflective elements and a fibre optic cable into which focused energy is directed to achieve a minimum target exit flux of  $85 \text{ W/cm}^2$ . Optical characterisation of the elements show surface slope errors between 5.67 mrad and 2.90 mrad. Computational ray trace results incorporating realistic error values show that for a worst case error scenario, FOCUS can provide flux levels exceeding  $130 \text{ W/cm}^2$  at fibre optic outlet. To validate the theoretical ray trace results, a flat plate calorimeter was constructed to measure the high-flux solar measurements. The calorimeter comprises a stainless steel outer body and copper receiving plate housed in a ring of insulating nylon. Energy absorbed by the water flow and external losses due to convection and radiation are predicted. Comparing energy balance results with that of the ray trace analysis shows FOCUS will perform at 142% of its theoretical ray trace value, assuming a conservative optical analysis. An exit fibre optic flux of  $188.9 \text{ W/cm}^2$  is predicted, suggesting that FOCUS is capable of sintering lunar regolith for ISRU applications. The FOCUS testing programme will commence in November 2010 to validate theoretical results.

## Acknowledgments

The authors appreciate the guidance of Professors J. Bindon and W.H. Moolman. Clinton Bemont, Khulisile Kunene and Michael Constantino are thanked for their assistance. OPTIS, Durban University of Technology and the University of Stellenbosch's Centre for Renewable and Sustainable Energy Studies (CRSES) are thanked for their support. This work is supported by the National Research Foundation of South Africa and the Eskom TESP program.

## References

- Ballestrín, J., Ulmer, S., Morales, A., Barnes, A., Langley, L.W. and Rodriguez, M. (2003) "Systematic error in the measurement of very high solar irradiance" *Solar Energy Materials and Solar Cells* Vol. 80, pg. 375-381.
- Ballestrín, J., Estrada, C.A., Rodríguez-Alonso, M., Pérez-Rábago, C., Langley, L.W. and Barnes, A. (2006) "Heat flux sensors: Calorimeters or radiometers?" *Solar Energy* Vol. 80, pg. 1314-1320.
- du Clou, S. Brooks, M.J., Bogi, B., Lear, W.E., Sherif, S.A. (2010) "Modeling of transient ejector performance with application to a pulse refrigeration system," presented at International Energy Conversion Engineering Conference (IECEC), AIAA.
- Estrada, C.A., Jaramillo, O.A., Acosta, R. and Arancibia-Bulnes, C.A. (2007) "Heat transfer analysis in a calorimeter for concentrated solar radiation measurements" *Solar Energy* Vol. 81, pg. 1306-1313.
- Feuermann, D., Gordon, J.M. and Huleihil, M. (2002) "Solar fiber-optic mini-dish concentrators: First experimental results and field experience" *Solar Energy* Vol. 72, No. 6, pg. 459-472.
- Incropera, F.P., Dewitt, D.P., Bergman, T.L. and Lavine, A.S. (2007) *Fundamentals of heat and mass transfer* 6<sup>th</sup> ed. USA. Wiley.



Jaramillo, O.A., Pérez-Rábago, C.A., Arancibia-Bulnes, C.A. and Estrada, C.A. (2008) "A flat-plate calorimeter for concentrated solar flux evaluation" *Renewable Energy* Vol. 33, pg. 2322-2328.

Kribus, A., Zik, O. and Karni, J. (2000) "Optical fibers and solar power generation" *Solar Energy* Vol. 68, No. 5, pg. 405-416.

Kumler, J.J. and Calwell, J.B. (2007) "Measuring surface slope error on precision aspheres" presented at SPIE Optics and Photonics.

Mouzouris, M. and Brooks, M. J. (2009) "Nonimaging solar thermal collector for high temperature terrestrial and space applications" presented at SPIE Optics and Photonics, San Diego, CA.

Mouzouris, M. and Brooks, M. J. (2009) "Misalignment effects in a point focus solar concentrator" presented at ISES Solar World Congress.

Mouzouris, M. and Brooks, M. J. (2010) "Construction of a composite material solar concentrator for high heat flux applications" presented at International Energy Conversion Engineering Conference (IECEC), AIAA.

Nakamura, T. and Senior, C. L. (2008) "Solar Thermal Power for Lunar Materials Processing" *Journal of Aerospace Engineering ASCE*, pg. 91-101.

Pérez-Rábago, C.A., Marcos, M.J., Romero, M. and Estrada, C.A. (2006) "Heat transfer in a conical cavity calorimeter for measuring thermal power of a point focus concentrator" *Solar Energy* Vol. 80, pg. 1434-1442.

Pregger, T., Graf, D., Krewitt, W., Sattler, C., Roeb, M. and Moller, S. (2008) "Prospects of solar thermal hydrogen production processes" *International journal of hydrogen energy*, pg. 4256-4267.

Vasylyev, V. and Vasylyev, S. (2002) "Expected optical performances of novel type multi-element high-heat solar concentrators" presented at American Solar Energy Society, Solar Conference.